Metal-Binding Affinity of the Transmembrane Site in ZntA: Implications for Metal Selectivity†

Junbo Liu, Sabari J. Dutta, Ann J. Stemmler, and Bharati Mitra*

Department of Biochemistry and Molecular Biology, School of Medicine, Wayne State University, Detroit, Michigan 48201

Received September 9, 2005; Revised Manuscript Received November 14, 2005

ABSTRACT: ZntA, a P_{1B}-type ATPase, confers resistance specifically to Pb^{2+}, Zn^{2+}, and Cd^2 in *Escherichia coli*. Inductively coupled plasma mass spectrometry measurements show that ZntA binds two metal ions with high affinity, one in the N-terminal domain and another in the transmembrane domain. Both sites can bind monovalent and divalent metal ions. Two proteins, ΔN-ZntA, in which the N-terminal domain is deleted, and C59A/C62A-ZntA, in which the N-terminal metal-binding site is disabled by site-specific mutagenesis, can only bind one metal ion. Because C59A/C62A-ZntA can bind a metal ion at the transmembrane site, the N-terminal domain does not block direct access of metal ions to it from the cytosol. A third mutant protein, C392A/C394A-ZntA, in which cysteines from the conserved CPC motif in transmembrane helix 6 are altered, binds metal ions only at the N-terminal site, indicating that both these cysteines form part of the transmembrane site. The metal affinity of the transmembrane site was determined in ΔN-ZntA and C59A/C62A-ZntA by competition titration using a metal ion indicator and by tryptophan fluorescence quenching. The binding affinity for the physiological substrates, Zn^{2+}, Pb^{2+}, and Cd^{2+}, as well as for the extremely poor substrates, Cu^{2+}, Ni^{2+}, and Co^{2+}, range from 10^6-10^{10} M^{-1}, and does not correlate with the metal selectivity shown by ZntA. Selectivity in ZntA possibly results from differences in metal-binding geometry that produce different structural responses. The affinity of the transmembrane site for metal ions is of similar magnitude to that of the N-terminal site [Liu J. et al. (2005) *Biochemistry 44*, 5159−5167]; thus, metal transfer between them would be facile.

P-type ATPases transport metal ions across membranes against a concentration gradient by utilizing the energy liberated from ATP hydrolysis. During the reaction cycle, they form an acyl phosphate intermediate in which the γ-phosphate of ATP is transferred to an invariant aspartic acid residue. P_{1B}-type ATPases, also known as "heavy metal" or CPX-type ATPases, constitute one of five subgroups of P-type ATPases. They transport "soft" metal ions across membranes—metal ions that are relatively large and easily polarized (*1*−*3*). P_{1B}-type ATPases are widespread and found in organisms from bacteria to humans; they maintain homeostasis of essential trace metals and are part of resistance mechanisms to purely toxic metals. They have been shown to transport metal ions such as Pb^{2+}, Zn^{2+}, Cd^{2+}- (*4*−*6*), Co^{2+}(*7*), Cu^+ (*8*−*13*), Cu^{2+}(*14*), and Ag^+ (*15*). Menkes and Wilson diseases in humans are caused by mutations in two Cu^+-transporting P_{1B}-type ATPases (*8*−*10*). In *Escherichia coli*, resistance to toxic concentrations of Zn^{2+}, Cd^{2+}, and Pb^{2+} is mediated by ZntA, a P_{1B}-type ATPase that transports these metal ions out of the cytoplasm (*5*−*6*).

Most, but not all, P_{1B}-type ATPases have a soft-metal binding domain at the N-terminus, a feature that is distinctive of this particular subgroup of P-type ATPases (*1*−*3*, *16*−*19*). Co^{2+}-transporting ATPases are unusual in that they do not have a metal-binding N-terminal domain (*7*). Different P_{1B}-type ATPases have a variable number of these metal-binding sites in the hydrophilic N-terminal domain, ranging from one to six (*2*−*3*, *20*). The N-terminal domain of ZntA, ∼120 residues long, binds a single soft-metal ion with high affinity (Figure 1) (*19*). Zn^{2+} is bound at a solvent-exposed site, with the two Cys residues and either one or both carboxylate oxygens of the Asp residue of the conserved ^{56}GMDCAAC^{62} motif supplying ligands to the metal ion (Figure 1) (*21*). Mutagenesis studies indicate that the Pb^{2+}-binding site at the N-terminal domain requires additional ligand(s) from the less prevalent ^{29}CCX(D/E)XXC^{35} motif (Figure 1) (*19*). Studies from a number of laboratories have shown that the N-terminal domain is not essential for function (*22*−*26*). However, the presence of a functional N-terminal metal-binding domain serves to increase the overall rate of the transporter.

Metal ion specificity and selectivity in ZntA remains unchanged when the N-terminal metal site is absent (*22*). Thus, metal selectivity, specificity, and overall activity is determined by metal site(s) in the rest of the protein, which are expected to be of central importance in the function of the transporter. P_{1B}-type ATPases have eight transmembrane segments. The sixth segment has a highly conserved (C/S/T)P(C/H) motif at the center. This segment corresponds to

† This work was supported by a United States Public Health Service Grant GM-61689 (to B.M.) S.J.D. acknowledges partial support from an American Heart Association Postdoctoral fellowship.

* Address correspondence to this author at Department of Biochemistry and Molecular Biology, Wayne State University School of Medicine, 540 E. Canfield Avenue, Detroit, MI 48201. Phone: (313) 577-0040. Fax: (313) 577-2765. E-mail: bmitra@med.wayne.edu.

10.1021/bi051836n CCC: $33.50
Published on Web 12/21/2005

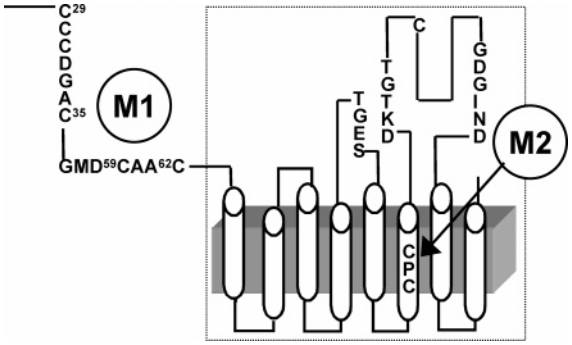

FIGURE 1: Schematic representation of ZntA showing the location of the two metal-binding sites, M1 and M2, in the N-terminal domain and in the transmembrane domain, respectively. The part enclosed in a dotted box represents the ΔN-ZntA construct. The positions of all nine cysteine residues in ZntA are shown.

the fourth transmembrane segment in P_2- and P_3-type ATPases, including SERCA1, the Ca^{2+}-ATPase from sarcoplasmic reticulum. The two residues flanking the proline are believed to supply ligands to soft-metal site(s) in the membrane; mutations of these cysteines result in complete loss of activity in copper-transporting ATPases (*25*−*27*). The number of high-affinity metal-binding sites in the transmembrane segment of P_{1B}-type ATPases, or their binding affinity for different metals, is not known. In this study, our goal was to characterize the transmembrane metal-binding site in ZntA, and most importantly, examine whether affinity for different metal ions is responsible for metal selectivity in ZntA and other P_{1B}-type ATPases.

We show that *wt*ZntA has two high-affinity metal-binding sites, one in the N-terminal domain and another in the transmembrane domain (Figure 1). Both sites are able to access and bind metal ion independently of each other. The transmembrane metal-binding site is essential because defects in this site result in an inactive protein unable to catalyze metal ion-dependent ATP hydrolysis. Metal-binding affinity of the transmembrane site was similar for both substrate and nonsubstrate metals, as well as monovalent and divalent ions. Thus, it appears that metal selectivity in ZntA does not result from differences in binding affinity; it is likely to be due to differences in coordination geometry of the metal ions that affect ATP hydrolysis. Given that the N-terminal and the transmembrane metal sites both have similar metal-binding affinity, metal transfer between them is expected to be facile. The rate enhancement provided by the N-terminal site could be due to a transfer of metal ion from it to the transmembrane site, which increases either the rate of binding or the release of metal ions from the latter.

EXPERIMENTAL PROCEDURES

Materials. Standard metal stock solutions were purchased from Sigma. Buffers and water used in the metal-binding experiments were deoxygenated by flushing with argon and passed through Chelex 100 (Sigma) to remove extraneous metal salts; the estimated final metal content of buffers was <50 nM. Standards for inductively coupled plasma mass spectrometry (ICP-MS) were from VWR.

Construction of C59A/C62A-ZntA and C392A/C394A-ZntA. Both double mutants were generated using the Quikchange Site-Directed Mutagenesis kit (Stratagene). The oligonucleotides (Integrated DNA Technologies, Coralville, IA) used for constructing the C59A/C62A-ZntA mutant were 5′-GTC-AGC-GGC-ATG-GAC-**GC**C-GC<u>G</u>-GCC-**GC**T-GCG-CGC-AAG-GTA-G-3′ and 5′-C-TAC−C<u>T</u>T-GCG-CGC-A**GC**-GGC-<u>C</u>GC-G**GC**-GTC-CAT-GCC-GCT-GAC-3′. Those used for constructing the C392A/C394A-ZntA mutant were 5′-CTG-ATT-GGC-**GC**C-CCG-**GC**T-GCG-TTA-GT<u>G</u>-AT<u>A</u>-TCA-ACG-CCT-G-3′ and 5′-C-AGG-CGT-TGA-<u>T</u>AT-<u>C</u>AC-TAA-CGC-A**GC**-CGG-G**GC**-GCC-AAT-CAG-3′; the altered bases for the mutations are indicated in boldface. Silent base changes (underlined base in the oligonucleotides) indicate restriction sites that were used to rapidly identify the presence of the desired mutations. The entire sequence of the mutant genes was verified by Automated DNA sequencing. The mutant genes were cloned in the pBAD/*Myc*-His C expression vector (Invitrogen) and expressed in strain LMG194(*zntA*::*cat*), with a hexahistidyl tag at the carboxy terminus, as previously described for ZntA (*28*) or in pBAD/*Myc*-His A, without a histidyl tag.

Sensitivity to Soft-Metal Salts. The sensitivity of LMG194, LMG194(*zntA*::*cat*) in which the entire *zntA* gene is deleted, as well as LMG194(*zntA*::*cat*) transformed with plasmids pZntA, pC59A/C62A-ZntA, or pΔN-ZntA[1] to metal salts was measured using a basal salts medium, pH 7.5, from which zinc salts were omitted (*29*). Cells were grown overnight and then diluted 50-fold in the same medium but containing metal salts as follows. For C59A/C62A-ZntA, the growth medium contained 10 μM lead acetate, 50 μM zinc chloride, or 5 μM cadmium chloride; growth at 37 °C was monitored by measuring the absorbance at 600 nm at fixed time intervals. For the C392A/C394A-ZntA mutant, cell growth was monitored after 24 h in medium containing 0−50 μM lead acetate, 0−100 μM zinc chloride, or 0−5 μM cadmium chloride.

Purification and Assay of C59A/C62A-ZntA and C392A/C394A-ZntA. The histidyl-tagged mutants were expressed by growing LMG194(*zntA*::*cat*) cells transformed with the appropriate plasmid at 37 °C in Luria Bertani medium followed by induction with 0.02% L-arabinose. Proteins were purified as described earlier, and the purity was checked by sodium dodecyl sulfate−polyacrylamide gel electrophoresis (*28*). This protein preparation was used for measurement of metal ion-dependent ATPase activity using a coupled assay with pyruvate kinase and lactate dehydrogenase (*28*). For assays in the presence of thiolates, the thiolate form of cysteine was added at a soft-metal ion/thiolate ratio of 1:1. Protein concentrations were determined using the bicinchoninic acid reagent with bovine serum albumin as the standard.

Formation of the acyl phosphate intermediate in the forward direction with [γ-^{32}P]ATP was assayed for purified proteins as described earlier (*30*). Phosphorylation in the reverse direction with [^{32}P]Pi was carried out as follows. Purified proteins (10 μg) pretreated with 2 mM DTT, were incubated in 100 μL of 50 mM Bis-Tris, pH 7.0, containing 25% dimethyl sulfoxide, 0.2% Triton X100 and 0.1% asolectin at 37 °C for 5 min, followed by a further incubation for 10 min after the addition of 30 μM metal salt solution. The reaction was initiated with 9 mM $MgCl_2$ and 20 μM

[1] Abbreviations: DDM: *n*-dodecyl-β-D-maltoside; ΔN-ZntA: a mutant of ZntA with residues 2−106 deleted; DTNB: 5,5′-dithiobis-(2-nitrobenzoic acid); EDTA: ethylenediaminetetraacetic acid; SDS−PAGE: sodium dodecyl sulfate−polyacrylamide gel electrophoresis.

[^{32}P]Pi. After 10 min, the reaction was stopped with 10% ice-cold TCA containing 1 mM NaH_2PO_4, incubated on ice for 10 min, and centrifuged for 10 min in a microcentrifuge. The pellet was washed three additional times with 10% ice-cold TCA containing 1 mM NaH_2PO_4 and resuspended in 100 μL of 25 mM H_3PO_4, pH 2.4, containing 5% SDS overnight at room temperature. Aliquots were directly counted in a scintillation counter.

Purification of the Non-Histidyl-Tagged Proteins for Metal-Binding Studies. For metal-binding studies, *wt*ZntA, C59A/C62A-ZntA, C392A/C394A-ZntA, and ΔN-ZntA were cloned in the pBAD/*Myc*-His A expression vector where the proteins are out-of-frame with the histidyl tag at the carboxy terminus. The proteins were expressed in strain LMG194-(*zntA*::*cat*), and the absence of the histidyl tag was confirmed by Western blotting using anti-His-tag antibody. The purification protocol was similar to that for the histidyl-tagged proteins until the isolation and detergent solubilization of the membranes. The membranes were solubilized with dodecyl maltoside and the extract incubated for 30 min at 4 °C with TALON metal affinity resin (BD Biosciences), preequilibrated in buffer containing 25 mM Tris, pH 7.0, 100 mM sucrose, 1 mM 2-mercaptoethanol, 150−500 mM NaCl, 1 mM phenylmethylsulfonyl fluoride, and 0.5 mM DDM. The resin was loaded onto a column and washed sequentially with the same buffer containing increasing concentrations of imidazole. The pure proteins were finally eluted with buffer containing 300 mM imidazole. Imidazole was immediately removed by gel filtration, and the protein-containing fractions were concentrated and stored at −70 °C in 25 mM Tris pH 7.0 containing 100 mM sucrose, 50 mM KCl, 1 mM phenylmethylsulfonyl fluoride, and 0.5 mM DDM. SDS−PAGE was used to check the purity of the non-histidyl-tagged proteins.

Free Thiol Quantitation. The number of free thiols in the reduced native and denatured proteins was quantified using a standard DTNB assay as described before (*19*, *31*).

Measurement of Metal-Binding Stoichiometry of ZntA, C59A/C62A-ZntA, C392A/C394A-ZntA and ΔN-ZntA by ICP-MS. The purified proteins in DDM were treated with 2 mM DTT and 5 mM EDTA at 4 °C for 1 h. DTT and EDTA were then removed by gel filtration with two consecutive Sephadex G-25 columns under anerobic conditions. The reduced apo-proteins (∼20 μM) were incubated with 3-fold excess molar concentrations of different metal salt solutions for 1 h at 4 °C. Excess metal salts were removed by repeated cycles of dilution and concentration. Control protein samples were prepared in the same way, except metal salts were not added to the incubation mixture. The buffer used in these experiments was 10 mM Bis-Tris, pH 7.0, containing 0.5 mM DDM; the counterion present in the buffer was nitrate. Protein samples were prepared for ICP-MS measurements by digesting with concentrated nitric acid at 70 °C for 1 h, followed by dilution. ICP-MS measurements were carried out as described earlier (*19*). The reported ICP-MS results are the average of three replicate experiments performed for each of two different protein sample preparations.

Relative Affinity of ΔN-ZntA and C59A/C62A-ZntA for Metal Using Mag-fura-2. The protocol for titration using metal indicators has been described earlier (*19*). Extraneous metal ions were removed from the buffers by passing over a Chelex 100 column. All buffers were deoxygenated and equilibrated with argon. Reduced apo-protein was prepared as described before and kept under argon for the duration of the experiment. For competition titration with mag-fura-2 (Molecular Probes), different aliquots of zinc chloride, lead acetate, cadmium acetate, or cupric chloride were added using a gastight syringe to 5−20 μM apo-protein and mag-fura-2 in 10 mM Bis-Tris, pH 7.0, in a sealed cuvette under argon. Metal-free mag-fura-2 has an absorbance maximum at 366 nm (ϵ = 29 900 $M^{-1}cm^{-1}$), which shifts to 325 nm in the metal-bound form (*32*). The stoichiometry and binding affinity of metals for ΔN-ZntA and C59A/C62A-ZntA were determined by monitoring the absorbance change at 366 nm.

Relative Metal Affinity of ΔN-ZntA by Monitoring Fluorescence Quenching. Fluorescence studies were carried out in a Perkin-Elmer model LS55 spectrofluorimeter. Metal-free, reduced ΔN-ZntA was prepared as described above. Titration with different metal salts was carried out with deoxygenated metal salt and protein solutions under argon at 20 °C in 10 mM Bis-Tris, pH 7.0. Aliquots of metal salt solutions were added from a gastight Hamilton syringe to reduced protein in a sealed cuvette. Following each addition, the solution was mixed well, and the fluorescence emission spectrum was collected. Excitation was at 290 nm. The effect of dilution following each addition of metal salt solution was taken into account.

RESULTS

In Vitro and in Vivo Activity of C59A/C62A-ZntA. The hydrophilic N-terminal domain of ZntA is not essential for activity or metal selectivity because a mutant of ZntA in which this domain was completely deleted, ΔN-ZntA, is active, although with 2−3-fold lower activity than *wt*ZntA (*22*). To test whether the difference in activity between *wt*ZntA and ΔN-ZntA was solely the result of the absence of the N-terminal metal-binding site or due to the deletion of the entire domain, we characterized C59A/C62A-ZntA, in which the N-terminal metal-binding site was knocked out by site-specific mutagenesis, but the N-terminal domain was still present. It was expressed using the same expression vector used for *wt*ZntA and ΔN-ZntA and purified using Ni^{2+}-affinity chromatography as described earlier (*28*, *22*). C59A/C62A-ZntA shows ATP hydrolysis activity that is significantly stimulated by Pb^{2+}, Zn^{2+}, or Cd^{2+} salts (*28*, *22*). Table 1 summarizes the kinetic parameters for C59A/C62A-ZntA for the ATPase activity at pH 7.0 and 37 °C; the data for *wt*ZntA and ΔN-ZntA are also included for comparison. The V_{max} for the Pb^{2+}-, Zn^{2+}-, and Cd^{2+}-dependent activity for C59A/C62A-ZntA was similar to ΔN-ZntA and 2−3-fold lower compared to *wt*ZntA for Pb^{2+} and Zn^{2+}. The apparent K_m values for the mutant protein were similar to that of ΔN-ZntA. The apparent K_m for Pb^{2+} is slightly lower for *wt*ZntA compared to that of the mutant proteins. The thiolate form of cysteine in the assay buffer increased the ATPase activity of *wt*ZntA, although the apparent K_m values of the metal ions were higher in the presence of thiolates; this effect was especially striking for Cd^{2+} (*28*). This effect was observed to hold true for C59A/C62A-ZntA as well (Table 1). The reason thiolates increase the in vitro activity is not known; it is possible that the metal dithiolate complex is a better substrate. It is expected that in vivo metal ions would be chelated to small molecule thiols such as cysteine or glutathione.

Table 1: Kinetic Parameters Obtained for C59A/C62A-ZntA at 37 °C for the Metal Ions Pb^{2+}, Zn^{2+}, and Cd^{2+} in the Absence and in the Presence of the Thiolate Form of Cysteine Present at a Concentration Equal to the Soft-Metal Ion Concentration[a]

	ZntA[b]		ΔN-ZntA[b]		C59A/C62A-ZntA	
	V_{max}	apparent K_m	V_{max}	apparent K_m	V_{max}	apparent K_m
Pb^{2+}	584 ± 30	4.8 ± 0.9	319 ± 6	11.6 ± 0.8	358 ± 16	8.9 ± 0.4
Zn^{2+}	247 ± 13	10.3 ± 1.9	81 ± 7	9.3 ± 1.2	95 ± 8	8.0 ± 0.7
Cd^{2+}	57 ± 3	5.5 ± 1.2	66 ± 3	4.1 ± 0.6	65 ± 16	5.1 ± 0.9
Pb^{2+} + thiolate	2500 ± 70	166 ± 15	1095 ± 67	55 ± 11	1023 ± 32	68 ± 5
Zn^{2+} + thiolate	710 ± 28	96 ± 11	372 ± 6	42 ± 3	334 ± 7	36 ± 3
Cd^{2+} + thiolate	1025 ± 25	252 ± 16	388 ± 10	52 ± 5	419 ± 19	65 ± 12

[a]The assay buffer was 100 mM acetic acid, 50 mM Bis-Tris, and 50 mM triethanolamine, pH 7.0. The Mg^{2+} and ATP concentrations were 5 mM each. For comparison, data for ZntA and ΔN-ZntA are also included. V_{max} values are in nmol/(mg/min) and K_m values are in μM. [b] From ref *22*.

C59A/C62A-ZntA was similar to ΔN-ZntA with respect to in vivo activity, as well. We previously showed that strain LMG194(*zntA*::*cat*), in which the zntA gene is deleted, was hypersensitive to lead, cadmium, or zinc salts in the growth media (*19*). Metal resistance was restored when the strain carried a plasmid bearing the *wt*ZntA gene. A plasmid containing the Δ*N-zntA* gene was also able to restore metal resistance, although there was a distinct lag in growth rate of 6−12 h compared to *wt*ZntA (*19*). Growth patterns of LMG194(*zntA::cat*) containing *C59A/C62A-zntA* on a plasmid also showed a similar lag in growth rate compared to that of wtZntA in medium containing toxic levels of lead, zinc, and cadmium salts (data not shown). Thus, both ΔN-ZntA and C59A/C62A-ZntA were able to support growth under toxic metal conditions, but they were at a distinct disadvantage with respect to *w*tZntA.

Characterization of C392A/C394A-ZntA. The double mutant, C392A/C394A-ZntA, in which the two conserved cysteines in transmembrane domain 6 were altered to alanines, was expressed to a lesser extent than *wt*ZntA, and purified using similar protocols. These two cysteine residues are believed to supply ligands to the metal center in the transmembrane site (Figure 1). The purified protein showed no ATPase activity. It was unable to complement the lead, zinc, and cadmium sensitivity of the LMG194(*zntA*::*cat*) strain in vivo. The ability of the protein to form the acyl phosphate intermediate with ATP and inorganic phosphate was examined. *wt*ZntA, in common with all P-type ATPases, forms a covalent acyl phosphate intermediate as part of the reaction cycle. In the forward direction, formation of the intermediate requires the presence of soft-metal ions and ATP (*33*). Phosphorylation in the reverse direction with inorganic phosphate does not require metal ion binding. We showed earlier that *wt*ZntA could form the acyl phosphate intermediate with ATP; steady-state levels of acyl phosphate obtained with different metal ions followed the order: $Cd^{2+} > Zn^{2+} > Pb^{2+} \gg Cu^{2+} > Co^{2+} > Ni^{2+}$ with no intermediate detected for the monovalent ions, Cu^{+} or Ag^{+} (*30*). There was no intermediate detected with [γ-^{32}P]ATP for C392A/C394A-ZntA in the presence of Pb^{2+}, Zn^{2+}, or Cd^{2+} (data not shown). This result suggested that C392A/C394A-ZntA was defective in the first half of the overall reaction. To eliminate the possibility that the inactivity was simply due to an incorrectly folded protein, the ability of this mutant to catalyze the formation of the acyl phosphate intermediate in the reverse direction with [^{32}P]Pi was tested. Figure 2 shows that the mutant was competent in forming the intermediate in the absence of metal ions. However, unlike *wt*ZntA, the steady-state levels of the intermediate did not decrease upon addition of metal ions, suggesting that metal ions were unable to bind to the transmembrane site and shift the equilibrium to the E_1 conformation of the transporter. The E_1 conformation cannot be phosphorylated by inorganic P_i, but only by ATP (*33*).

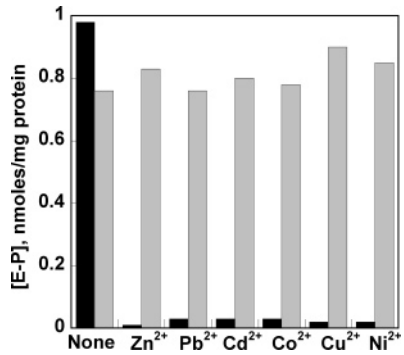

FIGURE 2: Acyl phosphate formation with purified *wt*ZntA (black bars) and C392A/C394A-ZntA (grey bars) using [^{32}P]-labeled sodium phosphate in the absence and in the presence of 30 μM different metal salt solutions.

Stoichiometry of Metal Ion Binding to wtZntA and Different Mutants Using ICP-MS. For experiments involving metal-binding studies, the proteins were expressed without any affinity tags and purified from detergent-solubilized membrane fractions. The purification protocol took advantage of the ability of the proteins to bind to metal-charged resin as long as they have at least one functional metal-binding site. Figure 3 shows an SDS−PAGE and corresponding Western blot of purified non-His-tagged *wt*ZntA, ΔN-ZntA and C392A/C394A-ZntA; also shown is purified His-tagged ZntA as a control. The non-His-tagged proteins could be effectively purified by this method to greater than 99%.

The metal-binding stoichiometry of *wt*ZntA, ΔN-ZntA, C59A/C62A-ZntA, and C392A/C394A-ZntA was determined using ICP-MS. *wt*ZntA could bind both substrate and nonsubstrate metal ions with a stoichiometry of 2 (Table 2). We showed earlier that the N-terminal domain of ZntA expressed separately has a single high-affinity metal-binding site (*19*). The results with *wt*ZntA therefore suggested that there is only one high-affinity metal-binding site in the rest of the protein. This was indeed the case since ΔN-ZntA, in which the N-terminal domain with its metal-binding site was deleted, could bind only one metal ion. This was also true for C59A/C62A-ZntA, in which the N-terminal domain was present, but the metal-binding site was knocked out (Table 2). The location of the metal-binding site in ΔN-ZntA and in C59A/C62A-ZntA was expected to be in the transmembrane region, since the CPC motif in the middle of trans-

FIGURE 3: 10% SDS−PAGE stained with Coomasie Blue showing purified proteins (upper panel) and the corresponding Western blot with an antibody against the histidyl tag (lower panel). Lanes: 1, molecular weight markers; 2, carboxy-terminal His-tagged *wt*ZntA; 3, non-His-tagged C59A/C62A-ZntA; 4, non-His-tagged ΔN-ZntA; 5, non-His-tagged C392A/C394A-ZntA.

membrane helix 6 is believed to provide two ligands to the metal. This is the case since C392A/C394A-ZntA, which has an intact N-terminal metal-binding site, was able to bind only one metal ion (Table 2), in contrast to *wt*ZntA.

Affinity of Zn^{2+}, Pb^{2+}, Cd^{2+}, and Cu^{2+} for the Transmembrane Site Using mag-fura-2. Purified proteins were reduced with DTT and then maintained under anaerobic conditions following removal of excess reducing agents. The number of free cysteines was measured by the DTNB assay. ZntA has a total of nine cysteine residues, with six located in the N-terminal domain (Figure 1). ΔN-ZntA has only three cysteine residues, including the two in the CPC motif. The DTNB assay showed that ZntA and ΔN-ZntA had six and two free cysteines under nondenaturing conditions, respectively. Under denaturing conditions, nine and three free cysteines were obtained for ZntA and ΔN-ZntA, respectively. Thus, following reduction of the protein and removal of the reducing reagent, both proteins were fully reduced under our experimental conditions. Of the six cysteines in the N-terminal domain, four were accessible, a result also obtained earlier for the isolated N-terminal domain (*19*).

The affinity of the transmembrane site, M2, was determined in reduced ΔN-ZntA and C59A/C62A-ZntA for the metal ions, Zn^{2+}, Pb^{2+}, Cd^{2+}, and Cu^{2+}, by competition titration with the metal ion indicator, mag-fura-2. Mag-fura-2 forms a 1:1 complex with divalent metals and has been extensively used to measure the affinity of zinc-binding sites. On titrating a mixture of mag-fura-2 and protein with aliquots of metal salt, the absorbance at 366 nm due to the metal-free form of mag-fura-2 decreased as increasing amounts of metal ion was bound to protein. Figure 4 shows a typical titration of Pb^{2+} with mag-fura-2 and ΔN-ZntA. The data were replotted in Figure 5A as the decrease in absorbance at 366 nm versus Pb^{2+} concentration. The data were best fitted to eq 2.

$$E + M^{2+} \leftrightarrow E{\cdot}M^{2+} \quad (1)$$

$$K_E^M = \frac{[E{\cdot}M^{2+}]}{[E_{(free)}][M^{2+}{}_{(free)}]} \quad K_I = \frac{[I{\cdot}M^{2+}]}{[I_{(free)}][M^{2+}{}_{(free)}]}$$

$$K_B = \frac{[B{\cdot}M^{2+}]}{[B_{(free)}][M^{2+}{}_{(free)}]} \quad (2)$$

Equation 2 describes the association constant (K_E^M) of a single metal ion (M^{2+}) with ΔN-ZntA or C59A/C62A-ZntA (E), as well as the association constant (K_I) of mag-fura-2 (I) with metal ion and the association constant (K_B) of the buffer, Bis-Tris (B) with metal ion. Bis-Tris was chosen as buffer because it forms a stable and soluble complex with Pb^{2+} and prevents formation of lead oxide and other insoluble species. The association constant, K_B, for the binding of different metal ions to Bis-Tris is known (*34*). Pb^{2+} and Cu^{2+} have somewhat high affinity for Bis-Tris, 2.1×10^4 and 1.9×10^5 M^{-1}, respectively; the values for Zn^{2+} and Cd^{2+} are 240 and 300 M^{-1}, respectively. The association constants for ΔN-ZntA were calculated for the different metal ions using the software Dynafit (*35*). The excellent fit of the titration data in Figure 5A−D indicated that under equilibrium conditions, both ΔN-ZntA and C59A/C62A-ZntA have a single, tight metal-binding site (M2 in Figure 1), in agreement with the results from ICP-MS experiments. For binding to Pb^{2+}, K_E^{Pb}, was calculated to be $\sim 5-8 \times 10^9$ M^{-1} for ΔN-ZntA and C59A/C62A-ZntA (Table 3). Similar measurements were carried out for Zn^{2+} and Cd^{2+}, the other two physiological substrates for ZntA, as well as Cu^{2+}, which we have shown earlier to be a relatively poor substrate for ZntA (Figure 3B−D) (*30*). As shown in Table 3, the affinity of Zn^{2+} and Cd^{2+} for the transmembrane site was ∼ 10-fold lower, $1-6 \times 10^8$ M^{-1}. However, Cu^{2+}, which is a poor substrate for ZntA, has a similar affinity for the transmembrane site as Pb^{2+}, $\sim 2-4 \times 10^9$ M^{-1}. The affinity of the transmembrane site for the different metal ions was quite similar for both ΔN-ZntA and C59A/C62A-ZntA.

The value of the association constant of mag-fura-2 with Zn^{2+} (K_I in eq 2), determined by fluorescence methods, is known, 5×10^7 M^{-1} (*36*). We determined the association constant of mag-fura-2 with Zn^{2+}, Cd^{2+}, Pb^{2+}, and Cu^{2+} in 10 mM Bis-Tris, pH 7.0 at 20 °C, by direct metal ion titration during which we monitored the absorbance change at 366 nm (data not shown). The affinity of the buffer, Bis-Tris, was taken into account when fitting the data. Values of the association constant obtained for Zn^{2+}, Cd^{2+}, Pb^{2+}, and Cu^{2+} were 5.2×10^7, 2.5×10^7, 3.1×10^8, and 8.4×10^9 M^{-1}, respectively. For the fits shown in Figure 5, either these values were used directly, or in some cases, K_I was treated as a variable during the data fitting. When K_I was a variable, the values obtained for it were within 1−4-fold of the experimentally determined values.

Affinity of the Transmembrane Site in ΔN-ZntA for Different Metal Ions Using Direct Fluorescence Quenching. ZntA has a total of six tryptophan residues, five of which are located in ΔN-ZntA. The fluorescence emission due to

Table 2: Stoichiometry of Metal Bound to *wt*ZntA, ΔN-ZntA, C59A/C62A-ZntA, and C392/C394A-ZntA Using ICP-MS[a]

	zinc	lead	cadmium	cobalt	copper	mercury	nickel	silver
*wt*ZntA	2.2 ± 0.0	1.8 ± 0.1	1.9 ± 0.0	2.1 ± 0.3	1.8 ± 0.4	1.9 ± 0.0	1.9 ± 0.3	1.9 ± 0.3
ΔN-ZntA	1.0 ± 0.1	0.9 ± 0.1	1.0 ± 0.1	1.0 ± 0.1	1.1 ± 0.1	1.0 ± 0.1	0.9 ± 0.1	0.9 ± 0.0
C59A/C62A-ZntA	1.2 ± 0.1	0.9 ± 0.1	0.9 ± 0.2	0.9 ± 0.1	1.1 ± 0.1	1.0 ± 0.1	1.1 ± 0.0	0.8 ± 0.1
C392A/C394A-ZntA	1.2 ± 0.2	1.0 ± 0.1	1.0 ± 0.0	1.1 ± 0.1	1.0 ± 0.0	1.0 ± 0.1	1.1 ± 0.1	1.0 ± 0.1

[a] Metal bound and control samples were prepared as described in Experimental Procedures. The metal content of control samples was <0.1% of the protein molar concentration (for Zn^{2+}, control samples had <5% Zn^{2+} contamination). The reported values are averages of three independent sample measurements for each of two protein preparations.

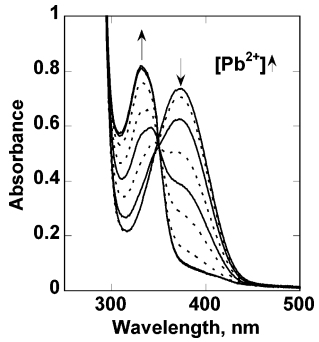

FIGURE 4: Representative spectra obtained during titration of 24 μM mag-fura-2 and 17 μM ΔN-ZntA with increasing concentrations of Pb^{2+} (0−57 μM) in 10 mM Bis-Tris, pH 7.0 and 20° C. The arrows denote the direction of the absorbance changes as increasing amounts of Pb^{2+} are added.

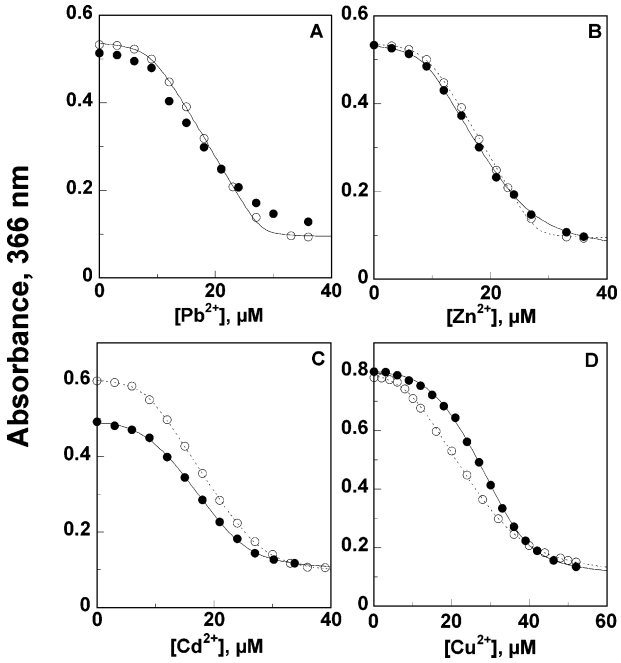

FIGURE 5: Plot of the absorbance changes at 366 nm when increasing concentrations of metal salt solutions were added to mag-fura-2 and C59A/C62A-ZntA (●) or ΔN-ZntA (○) in 10 mM Bis-Tris, pH 7.0 and 20 °C. Data were fitted to eq 2. (A) Pb^{2+}; (B) Zn^{2+}; (C) Cd^{2+}; (D) Cu^{2+}.

these five tryptophan residues is quenched ~15% on binding metal ion. This quenching of the tryptophan fluorescence provided a useful intrinsic tool to measure the affinity of different divalent metal ions. A titration of ΔN-ZntA with increasing concentrations of cadmium chloride is shown in Figure 6A; similar decreases in tryptophan fluorescence were observed for other divalent metal ions as well. The change in fluorescence intensity at 340 nm was plotted vs the cadmium chloride concentration in Figure 6B. The data were fit to the following equations (using Dynafit) that assumes a 1:1 binding model for the protein (E) and the buffer, Bis-Tris (B):

$$K_E^M = \frac{[E{\cdot}M^{2+}]}{[E_{(free)}][M^{2+}{}_{(free)}]} \quad K_B = \frac{[B{\cdot}M^{2+}]}{[B_{(free)}][M^{2+}{}_{(free)}]} \quad (3)$$

The affinity of Pb^{2+} and Zn^{2+}, the other two substrate metals for ZntA, as well as Cu^{2+}, Co^{2+}, and Ni^{2+}, metal ions that are very slow substrates for ZntA in vitro, was also determined using similar titration of the tryptophan fluorescence (data not shown). The association constants calculated from the titration data are summarized in Table 3. The values obtained for Pb^{2+}, Zn^{2+}, Cd^{2+}, and Cu^{2+} by this method were 4−10-fold lower than the values obtained by competition titration with mag-fura-2. These lower values arise because the only other metal ion competitor in these experiments, Bis-Tris, has a metal affinity that is many orders of magnitude lower than that of the protein; the effect is most pronounced for Zn^{2+} and Cd^{2+}, which have weak affinity for Bis-Tris. Thus, the values obtained by this method represent lower limits of affinity. However, a comparison of the affinity of ΔN-ZntA for different metals showed that there is no correlation between the affinity for a specific metal ion and the activity of the protein. Cu^{2+} and Ni^{2+} had the highest affinity, although Cu^{2+} and Ni^{2+} had extremely low activity (*30*). The affinity for Pb^{2+} was slightly lower; Pb^{2+} was the best substrate for ZntA (Table 1). Zn^{2+} and Cd^{2+} had 10−100-fold lower affinity than Pb^{2+}, although the activity was only 2−3-fold lower (Table 1). The affinity for Co^{2+}, a very weak substrate for ZntA, was significantly lower for the transmembrane metal-binding site in ΔN-ZntA than for the other metal ions tested (Table 3).

DISCUSSION

Although the N-terminal metal-binding site has been studied in isolated proteins for both ZntA as well as other P_{1B}-type ATPases, surprisingly little is known about the more important transmembrane metal-binding site(s) in these transporters. In this study, our goal was to characterize the transmembrane metal-binding site in ZntA. Additionally, we wanted to examine the importance of the N-terminal metal-binding site. We have shown earlier that deletion of the entire N-terminal domain of ZntA does not completely inactivate the transporter or alter its metal selectivity (*22*, *19*). The activity of the N-terminal-deleted mutant ΔN-ZntA is 2−3-fold lower than that of *wt*ZntA in vitro (*22*). In vivo, although it is able to complement the Pb^{2+}, Zn^{2+}, and Cd^{2+}-sensitivity of a *zntA*-deleted strain, it displays a lag in growth rate relative to *wt*ZntA in medium containing toxic concentrations of these salts (*19*). While these results showed that the

Table 3: Association Constants[a] for the Binding of Different Metal Ions to the Transmembrane Metal Site in ΔN-ZntA and C59A/C62A-ZntA

	lead	zinc	cadmium	copper	cobalt	nickel
C59A/C62A-ZntA[b]	$(7.7 \pm 3.3) \times 10^9$	$(2.2 \pm 0.5) \times 10^8$	$(1.0 \pm 0.2) \times 10^8$	$(4.1 \pm 0.8) \times 10^{10}$	nd	nd
ΔN-ZntA[b]	$(4.8 \pm 1.4) \times 10^9$	$(6.1 \pm 1.6) \times 10^8$	$(4.4 \pm 0.7) \times 10^8$	$(2.2 \pm 0.3) \times 10^{10}$	nd	nd
ΔN-ZntA[c]	$(1.2 \pm 0.5) \times 10^9$	$(1.3 \pm 0.8) \times 10^7$	$(3.8 \pm 1.2) \times 10^7$	$(2.9 \pm 1.1) \times 10^9$	$(3.1 \pm 0.4) \times 10^6$	$(2.9 \pm 2.1) \times 10^9$

[a] Units are in M^{-1}. Protein samples were prepared as described in Experimental Procedures. The reported values are averages of independent titrations with different protein preparations. nd, not determined. [b]Using competition titration with mag-fura-2. [c]By direct fluorescence quenching.

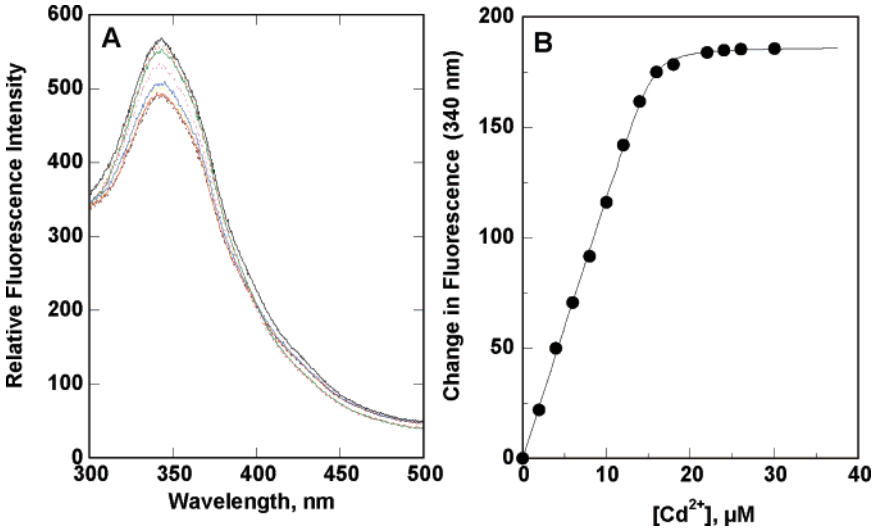

FIGURE 6: (A) Decrease in fluorescence emission when increasing concentrations of cadmium acetate were added to ~10 μM ΔN-ZntA in 10 mM Bis-Tris, pH 7.0 and 20 °C. The excitation wavelength was 290 nm. (B) Changes in fluorescence emission at 340 nm from panel A (excitation 290 nm) as a function of the added cadmium salt concentration. The data were fitted to eq 3.

N-terminal domain was not strictly necessary for activity and metal selectivity, it was not clear whether the differences from *wt*ZntA were due only to the absence of the N-terminal metal-binding site or whether deletion of the entire domain had additional effects. In particular, it was necessary to ensure that metal-binding site(s) in the transmembrane region were not affected by the absence of the N-terminal domain. Therefore, we characterized a different mutant, C59A/C62A-ZntA, in which the N-terminal domain was intact, but the metal-binding site was altered. C59A/C62A-ZntA closely resembles ΔN-ZntA, both in vitro and in vivo. Thus, the decrease in activity for ΔN-ZntA is the result of the loss of the N-terminal metal-binding site and not the deletion of the entire domain. Not surprisingly, the N-terminal domain is not conserved in all P_{1B}-type ATPases (*7*, *20*). In ZntA, the N-terminal metal-binding site increases the overall kinetics of the pump. This small increase in rate gives a competitive advantage in vivo and explains why it has been conserved in the ZntA subgroup of P_{1B}-type ATPases.

C392A/C394A-ZntA, in which the N-terminal site is unaltered, but where the transmembrane site is knocked out, is completely inactive. Since the loss in activity is not due to misfolding of the protein as shown by its ability to be phosphorylated in the reverse direction with inorganic phosphate, the metal-binding site in the transmembrane domain is essential for activity.

ICP-MS measurements on *wt*ZntA, ΔN-ZntA, C59A/C62A-ZntA, and C392A/C394A-ZntA clearly identified one high-affinity site at the N-terminus, M1, and a second in the transmembrane region, M2, with contributions from 392Cys and 394Cys in the middle of transmembrane helix 6 (Figure 1). This result shows that the large cytoplasmic domains containing the ATP binding and hydrolysis sites do not have additional high-affinity soft-metal binding sites, although it does not preclude residues from these domains from interacting with sites M1 or M2. The ICP-MS results also demonstrate that because both ΔN-ZntA and C59A/C62A-ZntA were able to bind metal ions at the transmembrane site, M2, this site can access metal ions directly from solution, in the presence and in the absence of the N-terminal domain. Thus, the N-terminal domain does not block access of the transmembrane site to metal ions; the ability of ΔN-ZntA to bind metal is not due to the exposure of the M2 site to the cytosol resulting from the deletion of the N-terminal domain. This observation also suggests that the N-terminal domain does not serve a negative regulatory role in ZntA.

Surprisingly, the transmembrane metal site, M2, can bind both monovalent and divalent metal ions with high affinity. Under the conditions of the ICP-MS experiments, only metal ions that bind with reasonably high affinity are measured. This was also the case for M1, the N-terminal site, as previously observed with the isolated N-terminal domain, and is supported in this study by the results with *wt*ZntA (*19*). Since both metal sites in ZntA are able to bind a wide variety of metals, they are both rather nondiscriminating. This is an unexpected observation, especially for the transmembrane site; we had expected this site to provide metal specificity and selectivity by not being able to bind nonsubstrate metals such as Ag^+ at all, and by binding weak substrate metals such as Co^{2+} and Ni^{2+} with low affinity. However, the ICP-MS results suggest that differences in metal affinity do not contribute to metal specificity. We have shown earlier that no ATPase activity is obtained with Ag^+ for ZntA (*28*); moreover, Ag^+ and Cu^+ cannot form the acyl

phosphate intermediate with ATP (*30*). These monovalent ions are, however, inhibitors of the ATPase activity. Taken together, these results suggest that the monovalent ions bind at the same site as the divalent ions but are unable to catalyze ATP hydrolysis.

Similar values of metal-binding affinity were obtained for the transmembrane site in C59A/C62A-ZntA and ΔN-ZntA, showing that metal affinity is not affected by the deletion of the N-terminal domain. The metal selectivity measured by the ATPase activity in ZntA does not correlate with metal-binding affinity. This lack of correlation between metal affinity and selectivity in ZntA, and perhaps other P_{1B}-type ATPases, is surprising but not unexpected. It was recently shown that the nickel-responsive transcription factor, NikR, binds a number of divalent metals—Co^{2+}, Ni^{2+}, Cu^{2+}, Zn^{2+}, and Cd^{2+}—with high affinity; in fact, it binds Cu^{2+} much more tightly than Ni^{2+} (*37*). However, the Ni^{2+}-NikR complex is more stable than complexes of NikR with other metals. It was suggested that the square planar geometry of Ni^{2+} in NikR produces a favorable allosteric effect that determines stability and leads to selectivity. The SmtB/ArsR family of metalloregulatory transcription factors also binds a number of metal ions with exceptionally high affinity (*38*). These unusually high affinities suggest that these proteins do not operate under themodynamic control, but rather under kinetic control in the cell, such that affinity would not be expected to play a role in selectivity. In fact, evidence from the Ni^{2+}- and Co^{2+}-sensing NmtR repressor from *Mycobacterium tuberculosis* showed that metal-binding affinity is not directly related to transcriptional response (*39*). On the other hand, the Cu^{+}-responsive regulator CueR responds to monovalent metal ions in the order $Ag^{+} > Cu^{+} \sim Au^{+}$, while it discriminates against binding divalent transition metals such as Zn^{2+} and Hg^{2+} because of constraints in binding geometry (*40*). The conclusion from these different studies is that for metal-responsive transcriptional factors, metal selectivity does not result from differences in thermodynamic affinity for divalent metal ions. Selectivity may result from specific coordination geometry that induces a certain conformation of the protein or from the specific nature of the intracellular metal ion concentrations.

The NMR structure of the N-terminal metal-binding site in ZntA with Zn^{2+} bound to it shows a tetrahedral coordination geometry (*21*), which is generally favored by Zn^{2+} and Cd^{2+}. Although structural information for the transmembrane site is not available, we expect that Zn^{2+} and Cd^{2+} will be bound with a tetrahedral geometry to this site as well. The geometry of Pb^{2+}, the best substrate for ZntA, bound to the M1 site or the M2 site is not yet known. Biochemical evidence indicates that Pb^{2+} binding at the M1 site is different from that of Zn^{2+} (*19*). It is possible that it binds with trigonal geometry, similar to the Cd^{2+}/Pb^{2+}-regulator CadC, which binds Cd^{2+} with tetrahedral coordination but Pb^{2+} with a trigonal structure (*41*−*42*). Ni^{2+} strongly prefers square planar geometry, while Cu^{2+} is frequently observed in a distorted tetrahedral or planar geometry. Thus, Ni^{2+} and Cu^{2+} may have somewhat different geometry of binding to the metal sites in ZntA compared to the substrate metals, Zn^{2+}, Cd^{2+}, and Pb^{2+}. Since the Co^{2+}-transporting ATPases appear to have a conserved (S/T)PC motif instead of the conserved CPC motif of the ZntA subfamily in transmembrane helix 6, it is likely that Co^{2+} binding to the CPC motif in ZntA induces different changes in structure compared to Zn^{2+} and Cd^{2+}. These differences in metal-binding geometry may produce different changes in protein structure that determine whether ATP will be hydrolyzed to form ADP and the acyl phosphate intermediate. Although Cu^{2+}, Co^{2+}, and Ni^{2+} bind with high affinity, they have extremely low acyl phosphate formation activity (*30*). Also, possibly, the linear geometry most likely adopted by monovalent metal ions such as Ag^{+} is incompatible with any reaction taking place. Future studies will focus on the structures adopted by different metal ions at the transmembrane site.

Earlier, we reported the affinity of the N-terminal metal-binding site in the isolated N-terminal domain, N1-ZntA, comprising residues 1−111 of ZntA (*19*, *43*). Association constants of $\sim 2 \times 10^7$, 5×10^7, and 2×10^8 M^{-1} were obtained for Pb^{2+}, Zn^{2+}, and Cd^{2+}, respectively, in 10 mM Bis-Tris. These values were relative to 10 mM Bis-Tris, pH 7.0 because the affinity of Bis-Tris for metal ions was not taken into account for the calculation in that study. If the affinity of the metal ions for Bis-Tris is used in the calculations as in eq 2 in this study, association constants of $\sim 2.2 \times 10^9$, 1.3×10^8, and 5.2×10^8 M^{-1} are obtained for Pb^{2+}, Zn^{2+}, and Cd^{2+} for the N-terminal metal-binding site in N1-ZntA. These values are similar to those obtained for the transmembrane site in this study. These metal affinity values suggest that physiologically ZntA transports metal ions out of the cytoplasm when the metal ion concentrations in the cytoplasm are in this range.

Given the similarity in metal ion affinity of the M1 and M2 sites, metal transfer between the two sites would be facile and under kinetic control. Since the presence of the N-terminal site appears to increase the overall rate of ZntA, its function may be to transfer metal ions to the M2 site, resulting in either a faster rate of metal binding to the M2 site or an accelerated rate of release from this site. Although it is not yet known which individual step(s) in the overall mechanism of ZntA is rate-limiting, earlier work with the acyl phosphate formation activity of ZntA suggested that metal binding and/or release could be the slow step(s) in the mechanism (*30*). Metal binding to the isolated N-terminal domain is quite fast, and release is quite slow (*43*). Rates of metal binding and release from the transmembrane site have yet to be measured. It has been proposed that in CopA from *Archaeglobus fulgidis*, the N-terminal site accelerates metal ion release (*26*). It is possible that for soft-metal ions, metal release is one of the slow steps, and metal binding to the N-terminal domain induces a strong negative cooperative effect on the transmembrane site, accelerating release of metal on the other side of the membrane.

Conclusion. *wt*ZntA has two high-affinity metal-binding sites, one in the N-terminal domain and a second in the transmembrane domain. The N-terminal site is not necessary for activity, although it increases the overall rate of the transporter. The transmembrane site is strictly required for activity. Both sites can bind monovalent and divalent soft-metal ions. The transmembrane site can access metal ions directly from the cytosol; the N-terminal domain does not block metal ions binding to it. The affinity of the transmembrane site for divalent metal ions was measured; the affinity for the three substrate metal ions, Pb^{2+}, Zn^{2+}, and Cd^{2+}, were similar to those of the N-terminal site. Therefore, metal transfer between the two sites would be facile. Association

constants for different divalent metal ions do not correlate with selectivity of metal ions transported. Cu^{2+} and Ni^{2+}, which are extremely poor substrates of ZntA, have the same affinity as Pb^{2+}, and slightly higher affinity than Zn^{2+} and Cd^{2+}. Similar observations have been made recently for metal-responsive transcriptional regulators. It is likely that in ZntA, metal selectivity stems from differences in binding geometry of different metal ions, which results in different structural responses that affect ATP hydrolysis and subsequent catalytic steps.

REFERENCES

1. Lutsenko, S., and Kaplan, J. H. (1995) Organization of P-type ATPases: Significance of structural diversity, *Biochemistry 34*, 15607−15613.
2. Solioz, M., and Vulpe, C. (1996) CPx-type ATPases: a class of P-type ATPases that pump heavy metals, *Trends Biochem. Sci. 21*, 237−241.
3. Axelson, K. B., and Palmgren, M. G. (1998) Evolution of substrate specificities in the P-Type ATPase superfamily, *J. Mol. Evol. 46*, 84−101.
4. Nucifora, G., Chu, L., Misra, T. K., and Silver, S. (1989) Cadmium resistance from *Staphylococcus* aureus plasmid pI258 cadA gene results from a cadmium-efflux ATPase, *Proc. Natl. Acad. U.S.A. 86*, 3544−3548.
5. Rensing C., Mitra B., and Rosen B. P. (1997) The *znt*A gene of *Escherichia coli* encodes a Zn^{2+}-translocating P-type ATPase, *Proc. Natl. Acad. Sci. U.S.A. 94*, 14326−14331.
6. Rensing, C., Sun, Y., Mitra, B., and Rosen, B. P. (1998) Pb^{2+}-translocating P-type ATPases, *J. Biol. Chem. 273*, 32614−32617.
7. Rutherford, J. C., Cavet, J. S., and Robinson, N. (1999) Cobalt-dependent transcriptional switching by a dual-effector MerR-like protein regulates a cobalt-exporting variant CPx-type ATPase, *J. Biol. Chem. 274*, 25827−2832.
8. Mercer, J. F., Livingston, J., Hall, B., Paynter, J. A., Begy, C., Chandrasekharappa, S., Lockhart, P., Grimes, A., Bhave, M., Siemieniak, D., et al. (1993) Isolation of a partial candidate gene for Menkes disease by positional cloning, *Nat. Genet. 3*, 20−25.
9. Vulpe, C., Levinson, B., Whitney, S., Packman, S., and Gitschier, J. (1993) Isolation of a candidate gene for Menkes disease and evidence that it encodes a copper-transporting ATPase, *Nat. Genet. 3*, 7−13.
10. Bull, P. C., Thomas, G. R., Rommens, J. M., Forbes, J. R., and Cox, D. W. (1993) The Wilson disease gene is a putative copper transporting P-type ATPase similar to the Menkes gene, *Nat. Genet. 5*, 327−337.
11. Odermatt, A., Suter, H., Krapf, R., and Solioz, M. (1993) Primary structures of two P-type ATPases involved in copper resistance in *Enterococcus hirae*, *J. Biol. Chem. 268*, 12775−12779.
12. Mandal, A. K., Cheung, W. D., and Arguello, J. M. (2002) Characterization of a thermophilic P-type Ag^{+}/Cu^{+}-ATPase from the extremophile *Archaeoglobus fulgidus*, *J. Biol. Chem. 277*, 7201−7208.
13. Rensing, C., Fan, B., Sharma, R., Mitra, B., and Rosen, B. P. (2000) CopA: an *Escherichia coli* Cu(I)-translocating P-type ATPase, *Proc. Natl. Acad. Sci. U.S.A. 97*, 652−656.
14. Mana-Capelli, S., Mandal, A. K., and Arguello, J. M. (2003) *Archaeoglobus fulgidus* CopB is a thermophilic Cu^{2+}-ATPase: Functional role of its histidine-rich-N-terminal metal binding domain, *J. Biol. Chem. 278*, 40534−40541.
15. Gupta, A., Matsui, K., Lo, J. F., and Silver, S. (1999) Molecular basis for resistance to silver cations in *Salmonella*, *Nat. Med. 5*, 183−188.
16. Lutsenko, S., Petrukhin, K., Cooper, M. J., Gilliam, C. T., and Kaplan, J. H. (1997) N-terminal domains of human copper-transporting adenosine triphosphatases (the Wilson's and Menkes disease proteins) bind copper selectively in vivo and in vitro with stoichiometry of one copper per metal-binding repeat, *J. Biol. Chem. 272*, 18939−18944.
17. DiDonato, M., Narindrasorasak, S., Forbes, J. R., Cox, D. W., and Sarkar, B. (1997) Expression, purification, and metal binding properties of the N-terminal domain from the Wilson disease putative copper-transporting ATPase (ATP7B), *J. Biol. Chem. 272*, 33279−33282.
18. Cobine, P. A., George, G. N., Winzor, D. J., Harrison, M. D., Mogahaddas, S., and Dameron, C. T. (2000) Stoichiometry of complex formation between copper(I) and the N-terminal domain of the Menkes protein, *Biochemistry 39*, 6857−6863.
19. Liu, J., Stemmler, A. J., Fatima, J., and Mitra, B. (2005) Metal-binding characteristics of the amino-terminal domain of ZntA: Binding of lead is different compared to cadmium and zinc, *Biochemistry 44*, 5159−5167.
20. Arguello, J. M. (2003) Identification of ion-selectivity determinants in heavy-metal transport P_{1B}-type ATPases, *J. Membr. Biol. 195*, 93−108.
21. Banci, L., Bertini, I., Ciofi-Baffoni, S., Finney, L. A., Outten, C. E., and O'Halloran, T. V. (2002) A new zinc-protein coordination site in intracellular metal trafficking: solution structure of the Apo and Zn(II) forms of ZntA(46−118), *J. Mol. Biol. 323*, 883−897.
22. Mitra, B., and Sharma, R. (2001) The cysteine-rich amino-terminal domain of ZntA, a Pb(II)/Cd(II)/Zn(II)-translocating ATPase from *Escherichia coli*, is not essential for its function, *Biochemistry 40*, 7694−7699.
23. Bal, N., Mintz, E., Guillain, F., and Catty, P. (2001) A possible regulatory role for the metal-binding domain of CadA, the *Listeria monocytogenes* Cd^{2+}-ATPase, *FEBS Lett. 506*, 249−252.
24. Fan, B., Grass, G., Rensing, C., and Rosen, B. P. (2001) *Escherichia coli* CopA N-terminal Cys(X)(2)Cys motifs are not required for copper resistance or transport, *Biochem. Biophys. Res. Commun. 286*, 414−418.
25. Fan, B., and Rosen, B. P. (2002) Biochemical characterization of CopA, the *Escherichia coli* Cu(I)-translocating P-type ATPase, *J. Biol. Chem. 277*, 46987−46992.
26. Mandal, A. K., and Arguello, J. M. (2003) Functional roles of metal binding domains of the *Archaeoglobus fulgidus* Cu(+)-ATPase CopA, *Biochemistry 42*, 11040−11047.
27. Bal, N., Wu, C. C., Catty, P., Guillain, F., and Mintz, E. (2003) Cd^{2+} and the N-terminal metal-binding domain protect the putative membranous CPC motif of the Cd^{2+}-ATPase of *Listeria* monocytogenes, *Biochem. J. 369*, 681−685.
28. Sharma, R., Rensing, C., Rosen, B. P., and Mitra, B. (2000) The ATP hydrolytic activity of purified ZntA, a $Pb^{2+}/Cd^{2+}/Zn^{2+}$-translocating ATPase from *Escherichia coli*, *J. Biol. Chem. 275*, 3873−3878.
29. Poole, R. K., Williams, H. D., Downie, J. A., and Gibson, F. (1989) Mutations affecting the cytochrome d-containing oxidase complex of *Escherichia coli* K12: identification and mapping of a fourth locus, cydD, *J. Gen. Microbiol. 135*, 1865−1874.
30. Hou, Z., and Mitra, B. (2003) Characterization of the metal specificity of ZntA from *Escherichia coli* using the acyl phosphate intermediate, *J. Biol. Chem. 278*, 28455−28461.
31. Riddles, P. W., Blakeley, R. L., and Zerner, B. (1979) Ellman's reagent: 5,5′-dithiobis(2-nitrobenzoic acid) − a reexamination, *Anal. Biochem. 94*, 75−81.
32. Walkup, G. K, and Imperiali, B. (1997) Fluorescent chemosensors for divalent zinc based on zinc finger domains. Enhanced oxidative stability, metal binding affinity, and structural and functional characterization, *J. Am. Chem. Soc. 119*, 3443−3450.
33. Inesi, G. (1985) Mechanism of calcium transport, *Annu. Rev. Physiol. 47*, 573−601.
34. Sigel, H. (1987) Isomeric equilibria in complexes of adenosine 5′-triphosphate with divalent metal ions. Solution structures of M(ATP)2-complexes, *Eur. J. Biochem. 165*, 65−72.
35. Kuzmic, P. (1996) Program DYNAFIT for the analysis of enzyme kinetic data: application to HIV proteinase, *Anal. Biochem. 237*, 260−273.
36. Simons T. J. (1993) Measurement of free Zn^{2+} ion concentration with the fluorescent probe mag-fura-2 (furaptra), *J. Biochem. Biophys. Methods 27*, 25−37.
37. Wang, S. C, Dias, A. V., Bloom, S. L., and Zamble, D. B. (2004) Selectivity of metal binding and metal-induced stability of *Escherichia coli* NikR, *Biochemistry 43*, 10018−10028.
38. Busenlehner, L. S., Pennella, M. A., and Giedroc, D. P. (2003) The SmtB/ArsR family of metalloregulatory transcriptional repressors: Structural insights into prokaryotic metal resistance, *FEMS Microbiol. Rev. 27*, 131−143.
39. Cavet, J. S., Meng, W., Pennella, M. A., Appelhoff, R. J., Giedroc, D. P., and Robinson, N. J. (2002) A nickel−cobalt-sensing ArsR−SmtB family repressor. Contributions of cytosol and effector binding sites to metal selectivity, *J. Biol. Chem. 277*, 38441−38448.
40. Changela, A., Chen, K., Xue, Y., Holschen, J., Outten, C. E., O'Halloran, T. V., and Mondragon, A. (2003) Molecular basis of

metal-ion selectivity and zeptomolar sensitivity by CueR, *Science 301*, 1383−1387.
41. Busenlehner, L. S., Cosper, N. J., Scott, R. A., Rosen, B. P., Wong, M. D., and Giedroc, D. P. (2001) Spectroscopic properties of the metalloregulatory Cd(II) and Pb(II) sites of *S. aureus* pI258 CadC, *Biochemistry 40*, 4426−4436.
42. Busenlehner, L. S., Weng, T. C., Penner-Hahn, J. E., and Giedroc, D. P. (2002) Elucidation of primary (alpha(3)N) and vestigial (alpha(5)) heavy metal-binding sites in *Staphylococcus aureus* pI258 CadC: evolutionary implications for metal ion selectivity of ArsR/SmtB metal sensor proteins, *J. Mol. Biol. 319*, 685−701.
43. Dutta, S. J., Liu, J., and Mitra B. (2005) Kinetic analysis of metal binding to the amino-terminal domain of ZntA by monitoring metal−thiolate charge-transfer complexes, *Biochemistry 44*, 14268−14274.

BI051836N